PROCEEDINGS OF SCIENCE

Integral/IBIS polarimetric results

P. Laurent
CEA-IRFU-APC
E-mail: plaurent@cea.fr

D. Götz*
CEA-IRFU-AIM
E-mail: dgotz@cea.fr

In complement to spectro-imaging observations, γ-ray polarimetry provides a unique insight into the geometry and magnetic configuration of compact γ-ray sources, such as neutron stars or black holes. These measurements were unsuccessful up to now because of intrinsic asymmetries in the detector response and of non-uniformities in the background dominated signals, which induce pseudo polarimetric signals, even from an unpolarized source. Due to the unprecedented spectral and timing capabilities of Integral, and thanks to its coded mask imaging technics, which efficiently suppresses most of the background contribution, we have measured linearly polarized emission from the brightest cosmic high energy sources. We were able to measure for the first time, at energies above 200 keV, a clear signal from several γ-ray sources such as the Crab pulsar, the black hole candidate Cygnus X-1, and a Gamma-Ray Burst, GRB 041219A. These observations have enabled us to put strong constraints on the physical process at work in these sources, and the achieved sensitivity opens a new window for polarimetric studies in the soft γ-ray regime.

The Extreme and Variable High Energy Sky - extremesky2011,
September 19-23, 2011
Chia Laguna (Cagliari), Italy

*Speaker.

PoS(Extremesky 2011)060

1. Introduction

γ-ray polarimetry has been possible with Compton telescopes since the 1970s. Photons that are Compton scattered between two detectors follow an azimuthal distribution around the source direction that allows to quantify the degree and direction of linear polarization because these photons are preferentially scattered in a plane at right angle to their incident electric vector. This measure was unsuccessful up to recently because of intrinsic asymmetries in the detector response and of non-uniformities in the large background signals. These defaults induce pseudo polarimetric signals, even from an unpolarized source, that limit the sensitivity to any detection. With its double layer of finely pixellated detectors [1], the IBIS telescope on board the Integral satellite [1] is well suited for polarimetry studies, between 200 keV and 5 MeV. In this paper, we will describe the polarimetry method we have developed, and present evidence for the detection of polarization from the Crab nebula, GRB 041219A, and Cygnus X–1 at energies above 200 keV.

2. Polarimetry with the Integral/IBIS Compton mode

Photons entering the INTEGRAL/IBIS telescope are Compton scattered in the first detector plane, ISGRI [2], at a polar angle θ from their incident direction and at an azimuth ψ from their incident electric vector. They are then absorbed in the second detector, PiCsIT [3]. The azimuthal profile $N(\psi)$, in Compton counts recorded per azimuth bin, follows:

$$N(\psi) = S[1 + a_0 cos(2\psi - 2\psi_0)] \tag{2.1}$$

for a source polarized at an angle PA = $\psi_0 - \pi/2 + n\pi$ and with a polarization fraction PF = a_0/a_{100}. The a_{100} amplitude is expected for a 100% polarized source. Unfortunately, the IBIS polarimetric capacities have not been calibrated on ground, due to the tight planning of the mission. We have then evaluated a_{100} to be 0.30 ± 0.02 for a Crab-like $E^{-2.2}$ spectrum between 200 and 800 keV, using GEANT3 Monte-Carlo simulations of IBIS with the GLEPS package[2] for polarization.

Events recorded in ISGRI and PiCsIT within the same time window of 3.8 μs are tagged as 'Compton' events, but do not all result from Compton scattering. Chance coincidences can occur between ISGRI and PiCsIT events independently coming from the source, the sky, or the instrumental background. These coincidences are generally called spurious events. Most of the 'Compton'-tagged events are due to background events that will be removed by the shadowgram deconvolution; 5% are due to a small fraction of spurious coincidences that must be removed with high accuracy because they induce a false source detection in the sky image; 2% come from true Compton events from the source.

The procedure we used to substract the spurious events contribution and measure the polarization is described in Forot et al. [4]. Confidence intervals on a_0 and ψ_0 are not given by the $N(\psi)$ fit to the data since the variables are not independent. They have been derived from the probability density distribution of measuring a and ψ from N_{pt} independent data points in $N(\psi)$ over a π period, based on Gaussian distributions for the orthogonal Stokes components [5]:

[1]Integral is an ESA project with instruments and science data center funded by ESA member states with the participation of Russia and USA. ISGRI has been realized and maintained in flight by CEA/Irfu with the support of CNES.

[2]GLEPS is a package for handling polarization in Geant 3 developed by Dr. Mark McConnell at University of New Hampshire, USA

PoS(Extremesky 2011)060

Table 1: Polarization angle and fraction with respect to the Crab pulsar phase ϕ

phase interval	polarization angle	polarization fraction	chance probability
P_1 and P_2	$70^\circ \pm 20^\circ$	$0.42^{+0.30}_{-0.16}$	33.5%
OP	$120.6^\circ \pm 8.5^\circ$	$> 0.72^a$	0.26%
OP and B	$122.0^\circ \pm 7.7^\circ$	$> 0.88^a$	0.10%
all	$100^\circ \pm 11^\circ$	$0.47^{+0.19}_{-0.13}$	2.8%

a : The lower limits for the polarization fraction are given at the 95 % confidence level.

$$dP(a,\psi) = \frac{N_{pt}\ S^2}{\pi\ \sigma_S^2} exp[-\frac{N_{pt}\ S^2}{2\ \sigma_S^2}[a^2 + a_0^2 - 2aa_0 cos(2\psi - 2\psi_0)]]\ a\ da\ d\psi \quad (2.2)$$

σ_S notes the error on the profile mean S. The errors on each a or ψ dimension are obtained by integrating dP(a,ψ) over the other dimension.

3. Crab observations

In this study, we use Integral observations of the Crab nebula between 2003 and 2007 for a total of 1.2 Ms. The pulsed lightcurve in the 200-800 keV band has been constructed with the Jodrell Bank ephemerides of the pulsar. We have considered four phase intervals for polarimetry studies : the two main peaks, the off-pulse interval and the bridge interval, dominated by the nebular emission. The interval boundaries were taken from [6] and were not adapted to enhance a possible signal. Table 1 and Fig. 1 show the results and illustrate the contrast between the modulation obtained for the nebular emission versus the flat profile of the pulsed emission.

There is indeed no significant indication of polarization in the pulsed peaks. The chance probability of a random fluctuation reaches 33.5 % and the signal shows no modulation at the 95 % confidence level over all angles. This behaviour is consistent with the radio and optical data where PF drops below 10 % as the angle largely flips within each peak [7]. Conversely, the chance is low that the modulation seen in the off-pulse emission above 200 keV be of random origin. The P(a,ψ) probability density yields a probability of 2.6 10^{-3} that a random fluctuation produces an amplitude a_0 larger than the recorded one. Adding the bridge and off-pulse data strengthens the signal and gives a chance probability of 10^{-3} that an unpolarized source produce this modulation. The observed modulation strongly differs from that of the spurious events recorded in the same Crab observations and from the instrumental asymmetries. So, the evidence for a strongly polarized signal holds against both statistical and systematic uncertainties. The polarization of the DC emission appears to be strong enough to still yield a marginal signal in the total Crab emission (see table 1).

The off-pulse-and-bridge emission is polarized at an angle of $122.0^\circ \pm 7.7^\circ$ which is fully consistent with the north-to-east angle $\psi = 124^\circ \pm 0.1^\circ$ of the pulsar rotation axis projected on the skyplane. At the 95 % confidence level, we find fractions $PF > 72\%$ and $PF > 88\%$ in the off-pulse and off-pulse-and-bridge emission, respectively, consistent, at the 95 % level, with an 77 % polarized signal along the pulsar rotation axis, which is the maximum polarization fraction

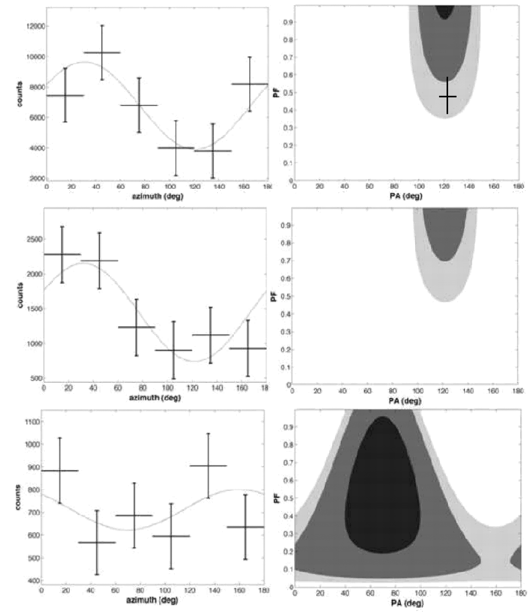

Figure 1: Azimuthal profile, modulation angle, PA, and fraction, PF, measured for the Crab data between 200 and 800 keV, in the off-pulse (top), off-pulse and bridge (middle), and two-peak (bottom) phase intervals. The error bars for the profile are at one sigma. The 68%, 95%, and 99% confidence regions are shaded from dark to light gray. The SPI result [8] is indicated in the top figure by a cross.

allowed for synchrotron radiation in a uniform magnetic field and from a power-law distribution of electrons with the spectral index p = 3.454 ± 0.026 recorded at these energies [6].

4. Observation of variable polarization from GRB 041219A

We used also the IBIS telescope on board the INTEGRAL satellite to measure the polarization of the prompt γ-ray emission of the long and bright gamma-ray burst GRB 041219A in the $200 - 800$ keV energy band [9]. We find a variable degree of polarization ranging from less than 4% over the first peak to $43 \pm 25\%$ for the whole second peak. Time resolved analysis of both peaks indicates a high degree of polarization, and the null average polarization in the first peak can be explained by the rapid variations observed in the polarization angle and degree. The azimuthal distributions of the GRB flux for the different time intervals are reported in figure 2.

Our results are consistent with different models for the prompt emission of GRB at these energies, but they favor synchrotron radiation from a relativistic outflow with a magnetic field which is coherent on an angular size comparable with the angular size of the emitting region ($\approx 1/\Gamma$) . Indeed this model has the best capabilities to maintain a high polarization level, and to produce the observed variability.

Finally, using a recent determination [10] of the distance of GRB041219A, and measuring the polarization properties of the emitted photons in two adjacent energy range, we were able to increase by 4 orders of magnitude the existing constraint on Lorentz invariance violations (LIV),

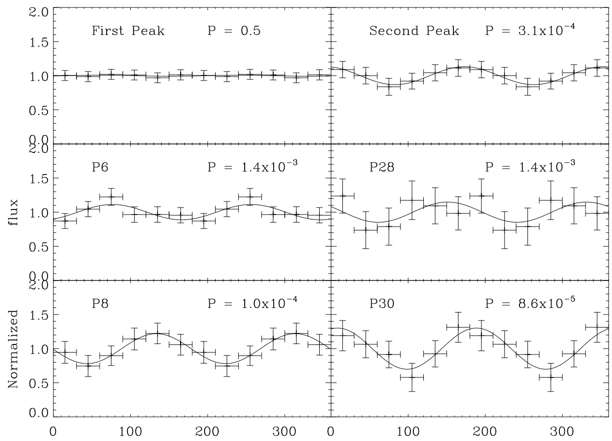

Figure 2: Polarigrams of the different time intervals that have been analyzed. For comparison purposes,the curves have been normalized to their average flux level.

arising from vacuum birefringence. Indeed, possible consequences of LIV are energy and helicity dependent photon propagation velocities. Turning the helicity dependence into a constraint on the coupling ξ of dimension 5 Lorentz violating interactions, that is of corrections of order k/M_{Pl} to the dispersion relations, this gives the very stringent constraint $\xi < 10^{-14}$ [12].

5. Observation of the Cygnus X–1 polarized high energy component

Cygnus X–1 is probably the best known black hole (BH) X-ray binary in our Galaxy. It is located around 2.1 kpc away from the Earth, and forms a binary system together with a high mass blue O star. It radiates mainly in the X-ray and soft gamma-ray domain and its X-ray luminosity is thought to come from accretion of the companion matter by the BH through the formation of an accretion disk. Finally, a compact radio jet is ejected from the vicinity of the BH, with a kinetic power similar to the source's bolometric X-ray luminosity (see [13] and references therein). The spectral measurements of the INTEGRAL/IBIS/Compton observations of Cygnus X-1 are shown in Figure 3 [13], where the X-ray/gamma-ray spectrum as obtained with the standard Integral/IBIS pipeline. Two high energy components are clearly seen, a cutoff power law component between 20 and 400 keV, reminiscent of a Compton-scattering induced spectrum, and a power law spectrum at higher energies of up to 2 MeV. These two components are signatures of two different high energy emission processes from the source, whose locations have not yet been constrained. A similar spectral feature has been recently observed by the SPI telescope [11], but with a lower amplitude. Cross-studies between IBIS and SPI are on-going in order to determine if this difference is due to inter-calibration problems, or to the MeV tail intrinsic variability.

Thanks to polarization measurements, we are now able to understand this gamma-ray emission geometry better. Indeed, the signal measured in the first energy band allowed for polarimetric study (250-400 keV) and shown in Figure 3 is consistent with a non-polarized signal with upper limit of

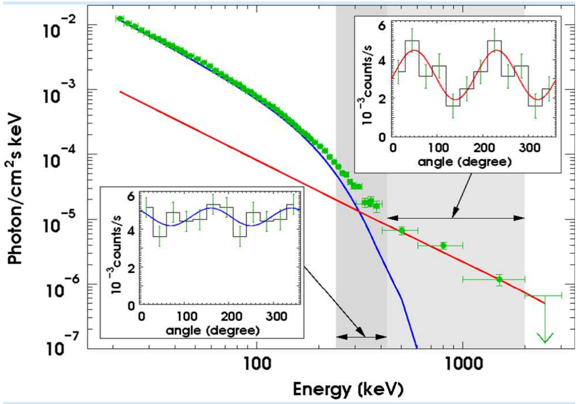

Figure 3: Spectra and polarigrams observed by the Integral/IBIS telescope from Cygnus X–1.

20% for the polarization fraction PF. This result agrees with what is expected from a zone where Compton scattering dominates. In contrast to the low polarization in the 250-400 keV band, the signal from the 400-2000 keV band in which the hard tail dominates is highly polarized (PF = $67 \pm 30\%$, see Figure 3). This result is no longer consistent with domination of Compton scattering, and such a high polarization fraction is probably the signature of synchrotron emission, e.g., from the jet already observed in the radio band.

References

[1] Ubertini, P., et al. 2003, A&A, 411, L131

[2] Lebrun, F., et al. 2003, A&A, 411, L141

[3] Labanti, C., et al. 2003, A&A, 411, L149

[4] Forot, M., Laurent P., Lebrun F., & Limousin O., 2007, ApJ, 668, 1259

[5] Weisskopf, M. C., 2006, Proc. of Neutron Stars and Pulsars, Bad Honnef, Germany

[6] Kuiper, L., Hermsen, W., Cusumano, G., Diehl, R., Schonfelder, V., Strong, A., Bennett, K., & McConnell, M. L. 2001, A&A, 378, 918

[7] Slowikowska, A., Kanbach, G., Kramer, M., & Stefanescu, A. 2008 Proc. of high time resolution astrophysics: The Universe at Sub-Second Timescales. AIP Conference Proceedings, 984, 51

[8] Dean, A.J., et al. 2008, Science, 321, 1183

[9] Götz D., Laurent P., Lebrun F., Daigne F.,Bosnjak Z., 2009, ApJ, 695, L208

[10] Götz D., Covino S., Hascoet R., Fernandez-Soto A.,, Daigne F., Moskovitch R., Esposito P., 2011, MNRAS 413, 2173

[11] Jourdain E., Roques J.P., Malzac J., 2011, this conference

[12] Laurent P., Götz D., Binétruy P., Covino S., Fernandez-Soto A., 2011, Phys.l Rev. D, 83, 12, 121301

[13] Laurent P., Rodriguez J., Wilms J., Cadolle Bel M., Pottschmidt K., Grinberg V., 2011, Science, 332, 6028, 438